Comparison of the soft-annihilation model of low-mass dilepton production with the data

V. Černý, P. Lichard, and J. Pišút
Department of Theoretical Physics, Institute of Physics and Biophysics, Comenius University, Bratislava, Czechoslovakia
(Received 15 September 1980)

Data on low-mass lepton pair production in hadron collisions are systematically compared with the predictions of the soft-annihilation model. In this model, lepton pairs are originated by the annihilations of quarks and antiquarks created during the collision. The surprisingly good qualitative and sometimes quantitative agreement indicates that this mechanism dominates the low-mass lepton pair production. Only further data on very-low-mass e^+e^- production can provide information about the relative amounts of soft subprocesses $q\bar{q}\to l^+l^-$ and $q\bar{q}\to l^+l^- + X$ (such as $q\bar{q}\to l^+l^-$ + gluon).

I. INTRODUCTION

Since its discovery in the Chicago-Princeton experiment,[1] the low-mass lepton pair production has been studied in numerous further experiments at different energies and by different beams. All evidence indicates that there exists a low-mass dilepton continuum not caused by well known sources such as Dalitz decays and the Bethe-Heitler process. Below, when speaking about low-mass lepton pairs, we shall have in mind the dileptons which remain after subtraction of these well known sources. The state of the art of low-mass dilepton production is well described in the recent review by Mikamo.[2] At present it seems that soft-annihilation models are in the best shape. In these models one assumes[3] that low-mass lepton pairs are originated by the annihilations of quarks (Q's) and antiquarks ($\bar{Q}$'s) created during the hadronic collision. This conclusion is based, however, on the comparison[2,4-6] of soft-annihilation-model predictions with only a very limited subset of the available data.

The purpose of this paper is to make a detailed comparison of the soft-annihilation model with the data. In this comparison we shall use our model,[4-6] but we believe that any model of this type has to lead to similar conclusions.

The paper is organized as follows. In the rest of the Introduction we shall describe the general features of the soft-annihilation model. In Sec. II, for the sake of completeness, we give some details of the model[4-6]. The comparison with the data is performed in Sec. III. Conclusions and comments are presented in Sec. IV.

Models which aim at describing the low-mass (LM) lepton pair production have to manage first to obtain the general qualitative features which can perhaps be summarized as follows.

(i) LM lepton pairs are produced with a relative rate 10^{-5}–10^{-4} with respect to single pions.

(ii) The LM dilepton continuum is roughly limited to the region below $M\sim 1$–2 GeV/c^2 and the shape of $d\sigma/dM$ is roughly independent of the energy and type of the beam. In the LM region the dilepton signal is much above the expectation of the naive extrapolation of the Drell-Yan model[7] which dominates at higher masses. The approximate beam-energy independence of $d\sigma/dM$ leads[8] to scaling properties which differ markedly from those typical for the Drell-Yan process.

(iii) The p_T and x_F inclusive distributions of the LM dilepton continuum, with masses above 500 MeV/c^2, are roughly similar to the inclusive spectra of mesons. Dileptons with masses below 400 MeV/c^2 are concentrated more at lower values of x_F and perhaps also at lower values of p_T.

These general features of the LM dilepton production are naturally accommodated by the soft-annihilation model,[3,4-6] provided that the constraints following from the space-time evolution[9] of hadron collisions are taken into account. We shall now discuss how this model accommodates items (i), (ii), and (iii).

(i) The incoming hadrons contain quarks, antiquarks, and gluons. If one takes a rough estimate of the number of Q's and $\bar{Q}$'s in the incoming hadrons and counts the Q's and $\bar{Q}$'s in the average multiparticle state a clear discrepancy is obvious. The recipe is to assume[3,10] that during the collision gluons are somehow converted to Q's and $\bar{Q}$'s and these finally recombine to hadrons. The original content of Q's and $\bar{Q}$'s is thus increased by a factor of about 5 and their recombination may provide the observed number of mesons, whereas their annihilation is able to give[3] a number of lepton pairs consistent with the observed 10^{-4}–10^{-5} dilepton/pion ratio.

(ii) According to the Bjorken-Gribov[9] parton-model picture of the space-time evolution of hadronic collisions [which remains presumably valid also in quantum chromodynamics (QCD)[9]], the hadronic collision evolves like an inside-outside cascade and different parts of the rapidity plot are excited at different times. This means that Q's and $\bar{Q}$'s created during the collision have

a chance to annihilate only if they are separated by a small rapidity gap. This means, however, that the mass of the $Q\bar{Q}$ system is small and leads naturally to a dilepton continuum concentrated at low masses. The energy independence of $d\sigma/dM$ means simply that the length of the rapidity region excited at a given time is independent of the energy of the collision.

(iii) If hadrons are originated by the recombination and LM lepton pairs by the annihilation of Q's and $\bar{Q}$'s separated by small rapidity gaps, then, quite naturally, the p_T and x_F spectra of directly produced mesons and LM dileptons are similar. Some possible sources of differences on a quantitative level still remain. In the annihilation one can think of the basic subprocesses (Fig. 1) as

$$Q\bar{Q} \to l^+ l^- \tag{1a}$$

as well as

$$Q\bar{Q} \to l^+ l^- + \text{gluon} \tag{1b}$$

or some other process of the latter type. In the same way, for the recombination of Q's and $\bar{Q}$'s to mesons, one can think of similar alternatives. When speaking below about recombination to mesons we shall assume[10] that the basic subprocess is a simple recombination and we shall consider (1b) as a possible correction to (1a), which is taken as a basic subprocess for the annihilation. It should be noted, however, that in subprocesses such as (1b) the gluon (or any system in $Q\bar{Q} - l^+ l^- + X$) takes away some momentum (both longitudinal and transverse) and dileptons produced via (1b) will tend to have lower x_F and p_T; this

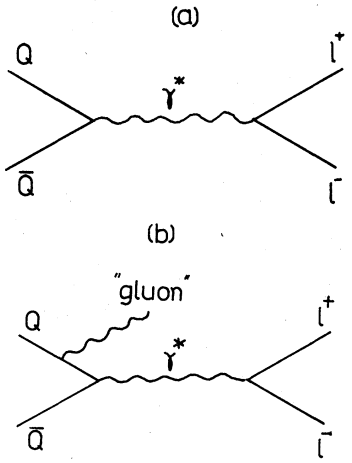

FIG. 1. Possible basic subprocesses in soft-annihilation mechanism: (a) direct annihilation, (b) annihilation with "gluon" emission. This diagram should be considered as a rough qualitative representation of diagrams $Q\bar{Q} \to l^+ l^- + X$.

may be relevant for some features observed in very-low-mass lepton pair production. The point is that (1a) and (1b) are kinematically very similar if the dilepton is energetic and the gluon is soft. If, however, the dilepton is soft (practically possible for e^+e^-, not for $\mu^+\mu^-$), the gluon is hard and (1a) and (1b) differ considerably.

It has to be stressed also that the quantitative formulation of the soft-annihilation models requires a simultaneous study of both multiparticle and LM dilepton production. In fact, the dilepton/hadron rate (and its energy dependence) and the predictions of the detailed shapes of x_F and p_T spectra of LM dimuons are to a large extent given by the distribution of Q's and $\bar{Q}$'s during the evolution of the collision. If one wants to have a model which has something to do with reality, then this distribution has to give a qualitative agreement (at least) with both the multiparticle and LM dilepton production.

In the present study we shall therefore use the same procedure for generating the distribution of Q's and $\bar{Q}$'s in $\vec{p}_T$ and p_L which we have used in our model of multiparticle production[10] in hadron collisions. As shown in Ref. 10, this distribution leads to reasonable agreement with the data on multiparticle production if hadrons are assumed to be produced simply by recombination of Q's and $\bar{Q}$'s separated by small rapidity gaps. In this way our distribution functions contain no free parameters. Having these distributions, we just allow the Q's and $\bar{Q}$'s separated by small rapidity gaps (this is managed by putting in by hand a function $\exp[-A(y_1 - y_2)^2]$ with $A \approx 1$ which allows only annihilations of Q's with $|y_1 - y_2| < A^{-1/2}$) to annihilate.

In the following section we shall describe the model in more detail.

II. THE MODEL OF SOFT ANNIHILATION DURING SPACE-TIME EVOLUTION OF THE COLLISION

We shall start here by discussing the assumed distribution of Q's and $\bar{Q}$'s during the collision; then we shall say a few words about the space-time evolution of the collision, and finally we shall present the method by which we have calculated the dilepton spectra.

During the hadronic collision the gluons are assumed to be converted to Q's and $\bar{Q}$'s and these in turn recombine to hadrons or (rather rarely) annihilate to lepton pairs. The distribution of Q's and $\bar{Q}$'s is thus changing in time. For practical reasons it is, however, more convenient to describe the distribution of Q's and $\bar{Q}$'s as if it were materialized all at once and then imagine that

it is materialized in different rapidity regions in different times. This permits us to respect some constraints which are of primary importance. Our ansatz thus corresponds to the distribution of Q's and $\overline{Q}$'s just after the conversion of gluons to Q's and $\overline{Q}$'s and before the recombination of Q's and $\overline{Q}$'s to hadrons.

The ansatz for the distribution fulfills the general constraints: (a) energy-momentum conservation, (b) transverse-momentum cutoff, and (c) valence quarks from colliding hadrons tend to have large momentum fractions. We shall use the following notation: V_T (V_P) = the number of the valence quarks of the target (projectile) particle, n = number of $Q\overline{Q}$ pairs generated during the collision, $N = 2n + V_T + V_P$ the total number of Q's and $\overline{Q}$'s after the gluon conversion and before the recombination, p_{Li} and $\vec{p}_{Ti}$ = longitudinal and transverse momenta of Q's and $\overline{Q}$'s, and x_i = momentum fractions in the c.m. system.

The probability for a given exclusive distribution of Q's and $\overline{Q}$'s was assumed[10] to have the following form:

$$dP_N(\vec{p}_1, \vec{p}_2, \ldots, \vec{p}_N) \sim G^n \delta\left(\sum_1^N \vec{p}_i\right) \delta\left(\sum_1^N E_i - \sqrt{s}\right) \exp\left(-\sum_1^V p_{Ti}^2/R_{\text{val}}^2 - \sum_{V+1}^N p_{Ti}^2/R_{\text{sea}}^2\right)$$

$$\times V(x_1, \ldots, x_V) \prod_1^N dy_i\, d^2p_{Ti}\,. \tag{2}$$

Here G is the factor regulating the average multiplicity. The factors for energy-momentum conservation are self-explanatory, as well as the factors for transverse-momentum cutoff. Note that we have used different values of the cutoff for valence and for sea Q's and $\overline{Q}$'s ($R_{\text{sea}} = 0.50$ and $R_{\text{val}} = 0.80$); this is motivated by our studies of multiparticle production. The expression

$$V(x_1, \ldots, x_{V_T}, x_{V_T+1}, \ldots, x_V) = \prod_1^V \sqrt{|x_i|} \prod_1^{V_T} \theta(-x_i) \prod_{V_T+1}^V \theta(x_i)$$

is the Kuti-Weisskopf[11] factor which gives larger probability to configurations in which valance quarks keep large momentum fractions. The constant G was determined at any energy by requiring that the average multiplicity of charged particles be consistent with the data. This value of $\langle n_{\text{ch}} \rangle$ was always calculated starting with the distribution in Eq. (2) and using the model described in Ref. 10. In assigning the quantum numbers to nonvalence quarks, we have suppressed the occurrence of strange quarks by a phenomenological factor $P_s/P_u = P_s/P_d \equiv \lambda = 0.5$, where P_u, P_d, and P_s are probabilities for up, down, and strange quarks, respectively. The parameters λ, R_{sea}, and R_{val} were kept fixed at all energies and for all the reactions at the values given above. Further comments about the distribution can be found in Ref. 10. The distributions [Eq. (2)] of Q's and $\overline{Q}$'s were generated by a Monte Carlo program on a computer.

If quarks within $dy_1 d^2p_{T1}$ are present in the excited region simultaneously with antiquarks within $dy_2 d^2p_{T2}$, and if they are both in a region of volume V_1 whose excitation lasts for time t_1, then the expected number of annihilations is

$$dn = dy_1 d^2p_{T1}\, dy_2 d^2p_{T2}\, |\vec{v}_Q - \vec{v}_{\overline{Q}}|\, \sigma_A^Q V_1 t_1 \times G_{Q\overline{Q}}(y_1, \vec{p}_{T1}, y_2, \vec{p}_{T2}) \frac{1}{V(y_1)V(y_2)}\,. \tag{3}$$

The joint probability $G_{Q\overline{Q}}(y_1, \vec{p}_{T1}, y_2, \vec{p}_{T2})$ is calculated from Eq. (2). The factor $1/V(y_1)V(y_2)$ [where $V(y)$ is the spatial volume of the excited system] is there because one needs the spatial densities of quarks. The volume is Lorentz contracted: $V(y) = V_0/\cosh y$.

Putting all the factors together we get[5] the final formula

$$\sigma_{l^+l^-} = \sigma_{\text{inel}}^{\text{hadr}} \left(\frac{ct_0}{V_0}\right) \sum_{Q\overline{Q}} \int \cdots \int dy_1 dy_2 d^2p_{T1} d^2p_{T2} G_{Q\overline{Q}}(y_1, \vec{p}_{T1}, y_2, \vec{p}_{T2}) |\vec{v}_Q - \vec{v}_{\overline{Q}}| \times \sigma_A^Q(y_1, \vec{p}_{T1}, y_2, \vec{p}_{T2}) \cosh y_1 \cosh y_2 w(y_1, y_2), \tag{4}$$

where $\sigma_{\text{inel}}^{\text{hadr}}$ is the inelastic hadronic cross section, which appears because by Eq. (3) we calculate the production of lepton pairs per hadronic collision. More details about the derivation of Eq. (4) can be found in Ref. 5.

The function $w(y_1, y_2)$ measures the probability that the quarks around y_1 and y_2 are excited simultaneously. We parametrized it rather arbitrarily

as $w(y_1, y_2) = \exp[-A(y_1 - y_2)^2]$. The parameter A fixes the length of the excited region in rapidity.

As discussed in the Introduction, we have considered two possible types of basic subprocesses: the direct annihilation

$$Q\bar{Q} \to l^+l^- \quad (\sigma_{A0}) \tag{5a}$$

and the annihilation with the emission of a gluon

$$Q\bar{Q} \to l^+l^- + \text{gluon} \quad (\sigma_{A1}). \tag{5b}$$

The cross sections for these two processes are denoted as indicated in parentheses and we have calculated them in a standard way (details are given in Refs. 5 and 6). The calculation of the former process is safe, whereas that of the latter is rather unreliable because one in fact uses the perturbative QCD outside its region of validity. We feel, however, that annihilations of the type (5b) with "gluon" representing "anything" may be important and wish to have a feeling for such contributions, so we have calculated the process (5b) in the lowest perturbative order and fixed the value of the gluon-quark-quark coupling constant arbitrarily at the value $\alpha_s = 0.5$.

When comparing model predictions with the data we shall present two types of results differing in the annihilation cross section inserted into Eq. (4):

$$\begin{aligned} &\text{Model I:} \quad \sigma_A = \sigma_{A0}, \\ &\text{Model II:} \quad \sigma_A = \sigma_{A0} + \sigma_{A1}. \end{aligned} \tag{6}$$

The constants entering Eq. (4) were fixed at the following values:

(i) $A = 1$. One expects that the length of the excited region is about one rapidity unit; values much lower than $A = 1$ are excluded by the data on $d\sigma/dM_{ll}$ at $M \gtrsim 2$ GeV/c^2. For A much lower than 1, $d\sigma/dM_{ll}$ would be much above the data. It is to be noted also that varying A from, say, 1 to 1.5 would have little influence on the dimuon production below the ρ mass.

(ii) The value of $\kappa = (ct_0/V_0)$ multiplying the cross section was fixed by comparing predictions following from Eq. (4) with the Chicago-Princeton data[1] on $pN \to \mu^+\mu^- + X$. In this way we have estimated

$$\kappa = 1.2 \times 10^{26}\ \text{cm}^{-2}, \quad \text{model I};$$

$$\kappa = 1.0 \times 10^{26}\ \text{cm}^{-2}, \quad \text{model II}.$$

The data on which this choice was based are shown in Table I. This value is quite reasonable, as we expect on physical grounds that $V_0 = a^3$, $a \approx ct_0 \approx 10^{-13}$ cm. One expects that the values of V_0 and ct_0 are fixed by the mechanism of the time evolution of the collision and should be roughly energy independent.

III. COMPARISON OF THE SOFT-ANNIHILATION MODEL WITH THE DATA

In this section we shall compare some of the available data on the LM dilepton production in hadron collisions with the predictions of our soft-annihilation model. A few remarks are in order. We made no attempts at fitting the data, although our model contains a few free parameters. We have fixed the values of these parameters partly by our preceding studies of multiparticle production, partly just by intuition (parameter A giving the length of the excited region), and partly by a rough comparison with the Chicago-Princeton data[1,12] (parameter $\kappa = ct_0/V_0$). These parameters were then held fixed for different beam particles and different energies. We believe that this is the only way in which one can make a reasonable qualitative comparison with the data.

The data will be compared with two models, the former containing only the direct soft annihilation $Q\bar{Q} \to l^+l^-$ (referred to as model I), the latter containig also the annihilation of the type $Q\bar{Q} \to l^+l^- + X$, where X is roughly represented by a gluon (referred to as model II).

We shall now pass to the comparison of model predictions with various sets of data.

Chicago-Princeton[1,12] data on dimuon production in pN collisions at 150 GeV/c. The total cross sections are compared with data in Table I. In fact, we need it, as described above, to fix the value of the parameter κ. More detailed comparison

TABLE I. Estimating the value of $\kappa = ct_0/V_0$ from the Chicago-Princeton data on the production of dimuons with $x_F > 0.15$ by pN collisions at 150 GeV/c. The comparison is somewhat complicated by the fact that the contributions from known sources (η and ω Dalitz decays, Bethe-Heitler) were not subtracted from the data and can only be roughly estimated to about 30–50 % of the cross section (Ref. 12, Fig. 49).

Mass interval	Data (known sources not subtracted) Ref. 1	Ref. 12	Model I with $\kappa = 1.2\ 10^{26}$ cm^{-2}	Model II with $\kappa = 1.0\ 10^{26}$ cm^{-2}
0.21–0.45 GeV/c^2	340 ± 70 nb	460 ± 55 nb	250 nb	320 nb
0.45–0.65 GeV/c^2	185 ± 37 nb	180 ± 22 nb	105 nb	110 nb

with this experiment was already done in Refs. 4 and 5 and we shall not repeat it here.

SLAC streamer-chamber data[13,14] on dimuon production in π^+p and π^-p collisions at 16 GeV/c. The authors present numbers of obtained events as a histogram in dimuon mass for dimuons with $x_F > 0.3$, and both π^-p and π^+p data are summed together to increase the statistics. They further give their acceptance as a function of dimuon mass and point out that their sample corresponds to 45.3×10^6 π^+p and 51.1×10^6 π^-p interactions. In order to compare our model predictions with their results we have calculated the number of events per bin according to the following formula:

$$n(M) = \Delta M\, A(M) \times (45.3 \times 10^6\, \rho_{\pi^+} + 51.1 \times 10^6\, \rho_{\pi^-}), \tag{7}$$

where $\Delta M = 0.03$ GeV/c^2 is the bin width, $A(M)$ denotes the acceptance, and

$$\rho_{\pi^\pm} = \frac{1}{\sigma_{\text{inel}}(\pi^\pm p)} \frac{d\sigma(\pi^\pm p \to \mu^+\mu^- X)}{dM}$$

are the cross sections for the production of dimuons with $x_F > 0.3$ in π^+p and π^-p interactions divided by the corresponding inelastic cross sections.

The data[13,14] are compared with our model in Fig. 2. The agreement in the low-mass region is acceptable, taking into account the statistics of the data. The ρ^0-meson peak from $\pi^\pm p \to \rho^0 + X$ followed by the $\rho^0 \to \mu^+\mu^-$ decay is of course not reproduced by our model since we have not included the ρ (and ω) production. The difference between models I and II is also rather small so that these data hardly make any distinction between the two models. This will be seen to be a common feature of dimuon data and it is also natural—the diagrams in Figs. 1(a) and 1(b) lead to kinematically different results only when the gluon takes away a considerable part of the energy. The total mass of the final-state system is, however, limited by the fact that only annihilations of $Q\bar{Q}$ pairs separated by small rapidity gaps are taken into account and the mass of the $\mu^+\mu^-$ system has to be rather large due to the muon rest mass. Because of that the gluon cannot be very energetic (in the c.m. system of the annihilating Q and $\bar{Q}$) and the propagator of the virtual photon in Fig. 1(b) cannot increase the contribution of this subprocess very much. Thus the diagram in Fig. 1(b) is actually suppressed by the three-body final state.

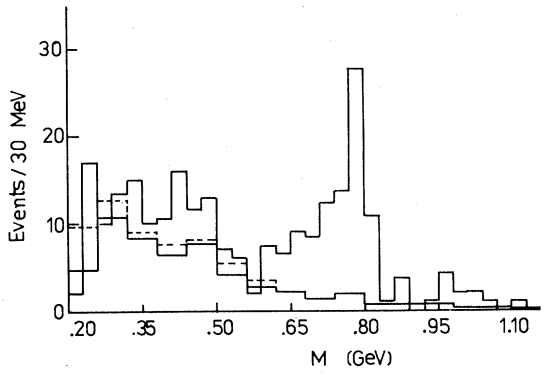

FIG. 2. Comparison of SLAC streamer-chamber results (Refs. 13,14) for the dimuon production in $\pi^\pm p$ collisions at 16 GeV/c for $x_F > 0.3$ with our model predictions. Narrow bins: Data (Ref. 13) after subtraction of the calculated hadron punchthrough and the most probable contribution from η and ω decays (taken from Ref. 14). Wide bins: Model calculations weighted by acceptance and normalized according to the total number of πp interactions as indicated in Eq. (7); solid: model I, dashed: model II.

The authors of Refs. 13 and 14 also present an interesting value of

$$\frac{\sigma(\pi^- p \to \mu^+\mu^- X)}{\sigma(\pi^+ p \to \mu^+\mu^- X)} = 1.28 \pm 0.23 .$$

Unfortunately the error is rather large and the ratio apparently also contains dimuons coming from ρ, ω, and η decays. Our model predicts the value 1.07. As will be seen below, in dielectron production this ratio can become a crucial test of the soft-annihilation model.

SLAC hybrid-bubble-chamber data[15] on dielectron production in π^+p and π^-p collisions at 18 GeV/c. *π^-p data* correspond to 5.2×10^5 inelastically produced charged pions. Taking the average charged-pion multiplicity as ~4 (about 2.2 for π^- and 1.6 for π^+), we estimate the number of inelastic π^-p interactions in the experiment as 1.3×10^5. The number of events per mass bin ΔM was then calculated from our model as

$$\frac{\Delta n}{\Delta M} = 1.3 \times 10^5 \times \frac{1}{\sigma_{\text{inel}}} \frac{d\sigma}{dM}$$

and this is compared with the data in Fig. 3. We present also the estimate (dots) of the ρ, ω, and η decays to e^+e^- production as well as the parametrization of the "excess" given in Ref. 15. The data on integrated e^+e^- production are compared with our model in Table II. It seems that model II is in somewhat better shape. This is also seen from Fig. 3 where we compare both models with the data on $d\sigma/dM_{e^+e^-}$. This indication is further corroborated by the data on $d\sigma/dp_T$ presented in Fig. 4. Experimentally the e^+e^- pairs are concentrated at low values of x_F. Only two pairs were seen with $|x_F| > 0.25$ (we expect 1.6 from model I and 2.2 from model II).

π^+p data correspond to 4.2×10^5 inelastically

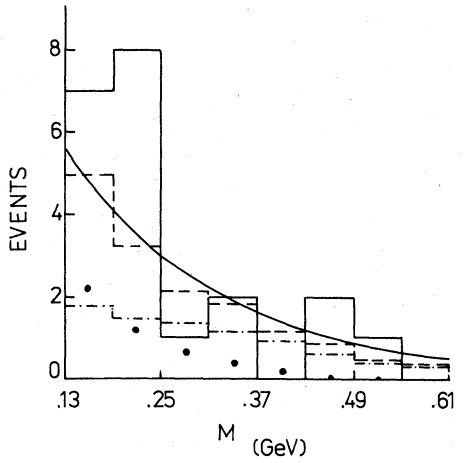

FIG. 3. SLAC hybrid bubble-chamber data (Ref. 15) for the dielectron production in $\pi^- p$ collisions at 18 GeV/c and our model predictions. The solid histogram represents the data and the solid curve is the "excess" [the difference between the data and the estimated number of e^+e^- pairs of known origin (dots)] parametrized by $C \exp(-m_{ee}/M)$, where we took (Ref. 15) $M = 0.195$ GeV/c^2 and we determined C from the number of events in the excess. The dashed (dash-dotted) histogram represents predictions of our model II (I).

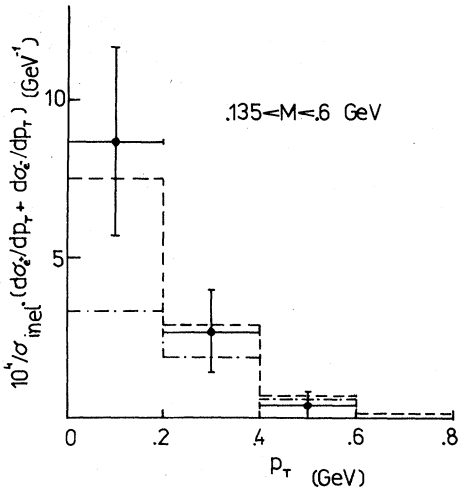

FIG. 4. Comparison of data (Ref. 15) for dielectron productions in $\pi^- p$ collisions at 18 GeV/c on the transverse-momentum distribution of electrons with our model. Dashed histogram: model II, dash-dotted: model I.

produced pions. Proceeding as in the previous case we obtain the expected number of dielectrons for the mass bin $0.135 < M_{e^+e^-} < 0.6$ GeV/c^2:

model I 5.2 events,

model II 9.5 events,

data[15] 1.5 events,

where the last line follows from 5 observed events in this mass range and 3.5 events expected from ρ, ω, and η decays. It seems therefore that the low rate for dielectron production in $\pi^+ p \to e^+e^- + X$ presents problems for our model and further data with higher statistics are required to clear up the issue.

Brookhaven-Yale data[16,17] on dimuon production in pN collisions at 28.5 GeV/c. The data are based on 74 acceptance-corrected events presented in a form of a histogram $\Delta n/\Delta M$. In order to compare them with the results following from our model, we have used Eqs. (5) from Ref. 16 which show that $\sigma(0.28 < x_F < 0.42, \text{all } M_{\mu\mu}) = 0.183$ μb and this number corresponds to 74 acceptance-corrected events. Setting $\sigma_{\text{inel}}(pN) = 31.8$ mb, we have

$$\frac{\Delta n}{\Delta M} = \frac{74}{0.183} \times 31.8 \times 10^3 \frac{1}{\sigma_{\text{inel}}} \frac{d\sigma_{\mu\mu}}{dM} .$$

In this way we have constructed the histograms presented together with the data in Fig. 5.

Chicago-Princeton data[12] on dimuon production

TABLE II. Comparison of integrated SLAC hybrid-bubble-chamber data[15] on e^+e^- production with model predictions.

$M_{e^+e^-}$ mass interval (GeV)	Number of events exp. excess	Model I	Model II
(0.067, 0.135)	7.0 ± 9.2	2.5	9.2
(0.135, 0.600)	16.1 ± 4.7	8.0	14.6

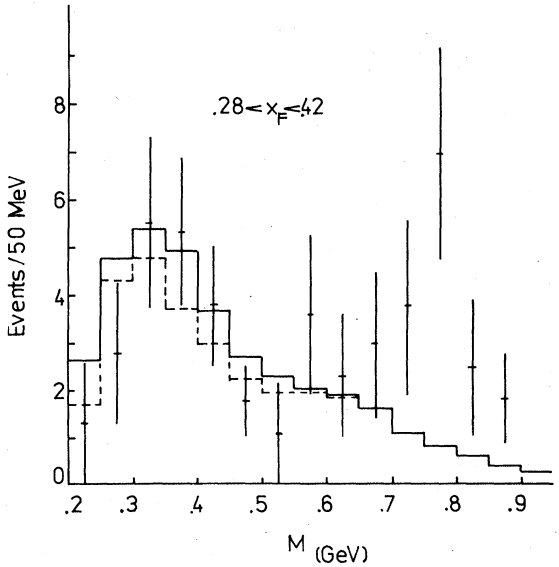

FIG. 5. Brookhaven-Yale data (Refs. 16,17) for dimuon production in pN collisions at 28.5 GeV/c compared with our results. Solid histogram—model II, dashed—model I.

by pN collisions at 225 GeV/c. These data provide probably the most detailed information. In Table III we compare integrated numbers of events in two dimuon mass intervals with our model. It has to be stressed that the data are not corrected for contributions from known sources, whereas model predictions contain only the soft annihilation. The true amount of experimental events due to unknown sources can be estimated from Fig. 6, which contains rather complete experimental information taken from Ref. 12 and our model predictions.

The dimuon spectra in x_F and p_T are presented for two mass bins in Figs. 7 and 8. Data were obtained from Ref. 12 and recalculated from a nuclear to nucleon target using $A^{0.75}$ dependence. The agreement is rather reasonable. It seems that the data slightly tend toward model II but, as already mentioned, the differences between the two models are very small for $\mu^+\mu^-$ production.

KEK double-arm-spectrometer data[2,18] on dielectron production in pN collisions at 13 GeV/c. The mass spectrum of dielectrons produced with $-0.05 \leq y \leq 0.05$ and recalculated per nucleon is compared with our model in Fig. 9. The agreement is satisfactory and comparisons with more detailed data from this experiment will be quite interesting. Model II seems to be in somewhat better shape but no final conclusions on this point can be made at present.

BEBC data on direct-electron production in 70 GeV π^-p interactions.[19] In this experiment, $15.2 \pm 4.4 e^+e^-$ pairs were observed with $M_{e^+e^-} > 0.135$ GeV/c^2. In our model (after appropriate weighting for the detection efficiency) we expect 6.3 and 10.9 events in models I and II, respectively. The agreement, taking into account the large experimental error, is satisfactory. The transverse-momentum spectrum of electrons is compared with our model in Fig. 10.

Search for direct-electron production in pp and pBe collisions at 12 GeV/c.[20] The aim of this experiment was mainly to study single electrons. However, the authors give also an estimate of the low-mass e^+e^- production,

$$\sigma(e^+e^-) < 0.25 \times 10^{-4}\sigma(\pi^0) \quad \text{for } M_{e^+e^-} < 0.1 \text{ GeV}/c^2.$$

TABLE III. Integrated dimuon production cross sections in nb ($x_F > 0.07$) by pN collisions at 225 GeV/c.

Mass interval (GeV/c^2)	Experiment (Ref. 12) (known sources not subtracted)	Model I	Model II
$0.21 < M_{\mu\mu} < 0.45$	871 ± 104	414	572
$0.45 < M_{\mu\mu} < 0.65$	319 ± 38	226	252

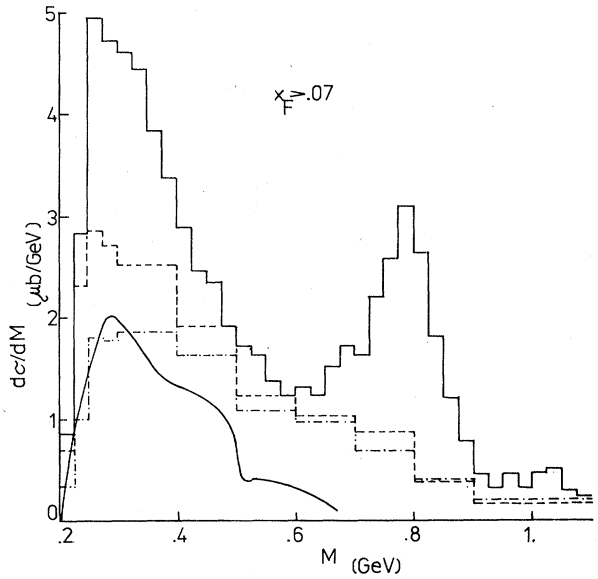

FIG. 6. Mass spectrum of dimuons produced in pN collisions at 225 GeV/c. The solid histogram represents the data (Ref. 12). The contribution from known sources (η and ω Dalitz decays, Bethe-Heitler process and $\eta \to \mu^+\mu^-$) estimated by Henry (Ref. 12) is denoted by the solid curve. Dashed histogram corresponds to model II, dash-dotted to model I. The data presented here were obtained from Fig. 49 and Table V in Ref. 12, and the recalculation to nucleon target was performed by using the $A^{0.75}$ dependence.

According to our model we expect

$$\sigma(e^+e^-) = 0.06 \times 10^{-4}\sigma(\pi^0), \quad \text{model I},$$

$$\sigma(e^+e^-) = 0.34 \times 10^{-4}\sigma(\pi^0), \quad \text{model II}.$$

It is clear that good data in this mass bin could be crucial for distinguishing between the two models.

IV. COMMENTS AND CONCLUSIONS

As shown by results presented in Sec. III, our soft-annihilation model of low-mass dilepton production is—at least—in a reasonable qualitative agreement with the available data. On this level the agreement is not caused by some specific features or specific selection of parameters, but it is directly due to the two basic assumptions of the model: (i) The main source of the LM dileptons is the annihilation of quarks and antiquarks created during the hadronic collision.[3,4] (ii) The constraints following from the space-time evolution[9] of the collision are taken into account and keep the LM continuum limited to the low-mass region.

At present there exist a few other models of low-mass dilepton production in hadronic collisions (Refs. 21–25 and for a review see Ref. 2). Some

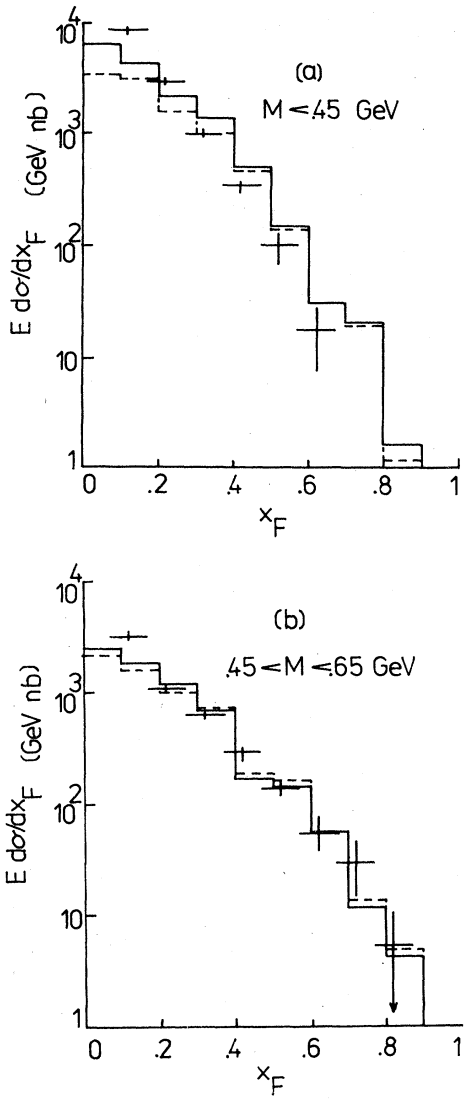

FIG. 7. Dimuon spectra in x_F for pN collisions at 225 GeV/c (Ref. 12) for two dimuon mass intervals: (a) $M<0.45$ GeV/c^2, (b) $0.45<M<0.65$ GeV/c^2. Solid histogram: model II; dashed: model I.

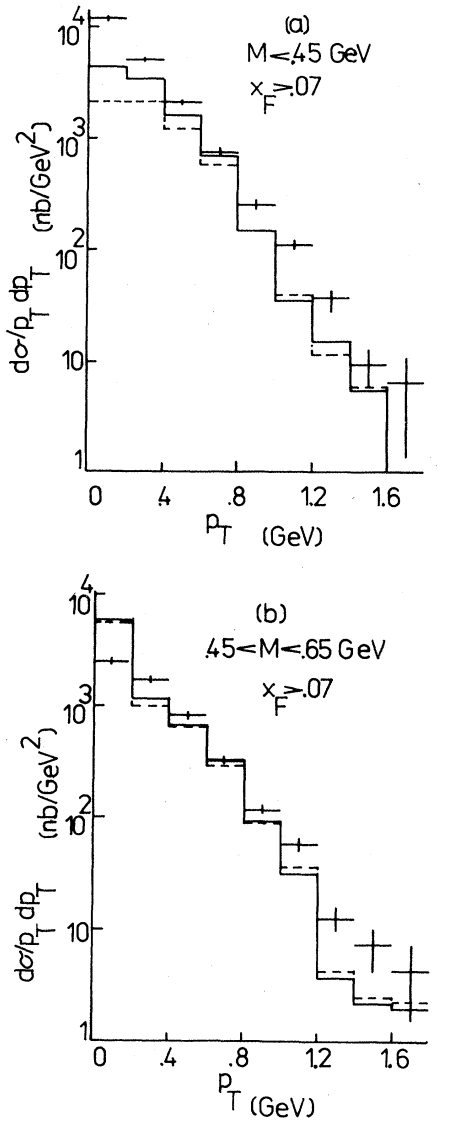

FIG. 8. Dimuon transverse-momentum spectra for pN collisions at 225 GeV/c for two dimuon mass intervals: (a) $M<0.45$ GeV/c^2, (b) $0.45<M<0.65$ GeV/c^2. Solid histogram: model II; dashed: model I.

of them[21-23] are based on pictures which to some extent overlap with the dynamics of the soft-annihilation model and some of their predictions will be thus similar to those following from our model. It would be very instructive if these models were systematically compared with the available data so that one could see clearly the similarities and differences.

An interesting question within the scheme of our model is the ratio of contributions of annihilation subprocesses of the two types (1a) and (1b). The resolution of this issue can come from more accurate data on the production of low-mass e^+e^- pairs with masses just above the pion mass and possibly also from the low-p_T behavior e^+e^- production (and of single electrons coming from such pairs).

As seen in Figs. 3 and 4, the data[15] from the low-mass region of e^+e^- production present serious indications of the relative importance of processes such as (1b). Low-p_T spectra of single electrons and of e^+e^- pairs are at present in a rather controversial state[2,20,26,27] and a clarification of the situation is desirable.

Another interesting point is the relative ratio of dielectron production in π^+p and π^-p collisions. Soft-annihilation models based on assumptions (i)

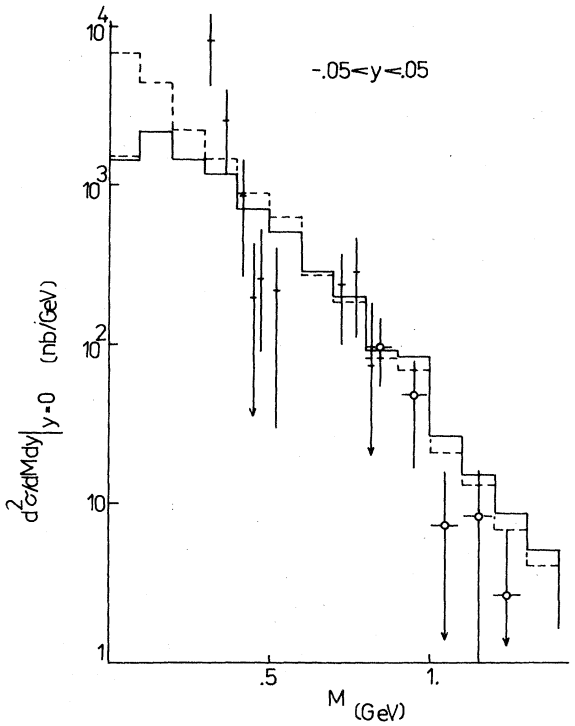

FIG. 9. Dielectron mass spectrum (Refs. 2,18) from pN collisions at 13 GeV/c compared with our model. Dashed histogram: model II; solid: model I.

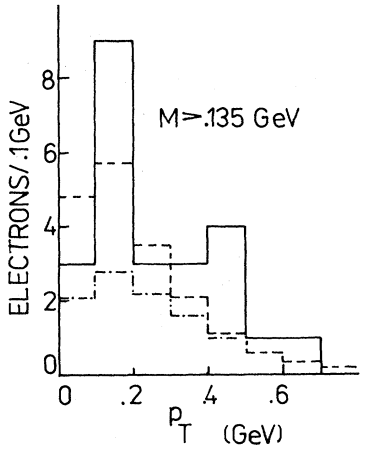

FIG. 10. Electron transverse-momentum spectrum for $\pi^- p$ collisions at 70 GeV/c [solid histogram (Ref. 19)] compared with our model. Dashed histogram: model II; dash-dotted: model I. We weighted the model calculations by the detection efficiency as given in Fig. 3 in Ref. 19.

and (ii) above make rather definite statements about this ratio. As seen from the discussion of the SLAC rapid-cycling hybrid-bubble-chamber data[15] in Sec. III, the present information on the low-mass e^+e^- production in π^+p collisions if confirmed in a higher statistics experiment could exclude soft-annihilation models.

Let us note finally that if the low-mass dileptons are really of a "hadronic origin," then the understanding of details of the dynamics of their production has to be done simultaneously with the study of multiparticle processes, and one has to compare a specific model of both processes with the data covering a broad energy range. If the hadronic origin of the LM dileptons is confirmed, then the LM dilepton production could become the simplest hadronic process and as such it could be useful for the analysis of more complicated processes of hadron production. This concerns not only hadron collisions but also reactions such as e^+e^- → hadrons and deep-inelastic scattering where one also expects[28] dileptons in the final state with a similar dilepton/hadron ratio as in the hadronic collisions.

[1]K. J. Anderson *et al.*, Phys. Rev. Lett. 37, 799 (1976); 37, 803 (1976).
[2]S. Mikamo, KEK Report No. 79-27, 1980 (unpublished).
[3]J. D. Bjorken and H. Weisberg, Phys. Rev. D 13, 1405 (1976).
[4]V. Černý, P. Lichard, and J. Pišút, Phys. Lett. 70B, 61 (1977).
[5]V. Černý *et al.*, Acta Phys. Pol. B9, 901 (1978).
[6]V. Černý *et al.*, Acta Phys. Pol. B10, 537 (1979).
[7]S. D. Drell and T.-M. Yan, Phys. Rev. Lett. 25, 316 (1970).
[8]V. Černý, Phys. Rev. D 18, 4345 (1978).
[9]J. D. Bjorken, in *Current Induced Reactions*, Vol. 56 of *Lecture Notes in Physics*, edited by J. Koerner *et al.* (Springer, Berlin, 1976), p. 93; in *Proceedings of the SLAC Summer Institute on Particle Physics;* edited by M. C. Zipf (SLAC, Stanford, 1973); V. N. Gribov, in *Elementary Particles*, proceedings of the First ITEP School on Theoretical Physics (Atomizdat, Moscow, 1973), Vol. I, p. 65. In what concerns the space-time evolution of hadron collisions, the quark-parton model and QCD lead most likely to very similar results. See, e.g., Yu. L. Dokshitzer and D. I. Dyakanov, in DESY Report No. L-Trans-234, 1979, material from the 14th Winter School of Leningrad Institute of Nuclear Physics, Leningrad, 1979 (unpublished), pp. 27-108; K. Konishi, CERN Report No. TH2897, 1980 (unpublished).
[10]V. Černý, P. Lichard, and J. Pišút, Phys. Rev. D 16, 2822 (1977); 18, 2409 (1978); 18, 4052 (1978); 20, 699 (1979).
[11]J. Kuti and V. F. Weisskopf, Phys. Rev. D 4, 3148

(1970).
[12]G. G. Henry, Ph.D. thesis, The University of Chicago, 1978 (unpublished).
[13]K. Bunnell *et al.*, Phys. Rev. Lett. 40, 136 (1978).
[14]R. F. Mozley, Stanford Report No. SLAC-PUB-2120, 1978 (unpublished).
[15]J. Ballam *et al.*, Phys. Rev. Lett. 41, 1207 (1978).
[16]W. M. Morse *et al.*, Phys. Rev. D 18, 3145 (1978).
[17]D. M. Grannan *et al.*, Phys. Rev. D 18, 3150 (1978).
[18]S. Naito *et al.*, contribution to the 1979 INS Symposium on Particle Physics in the GeV Region, Tokyo (unpublished), quoted in Ref. 2.
[19]R. Barloutand *et al.*, Rutherford Laboratory Report No. RL-80-003, 1980 (unpublished).
[20]Y. Makdisi *et al.*, Phys. Rev. Lett. 41, 367 (1978).
[21]J. Ranft and G. Ranft, Phys. Lett. 62B, 57 (1976).
[22]E. V. Shuryak, Yad. Fiz. 28, 796 (1978) [Sov. J. Nucl. Phys. 28, 408 (1978)]; Phys. Rep. 61, 71 (1980).
[23]T. Adachi and I. Yotsuyanagi, Phys. Rev. D 23, 1106 (1981).
[24]T. Goldman, Minh Duong-van, and R. Blankenbecler, Phys. Rev. D 20, 619 (1979).
[25]I. H. Dunbar, Phys. Rev. Lett. 41, 210 (1978); J. Walcock, W. N. Cottingham, and I. H. Dunbar, Nucl. Phys. B145, 85 (1978).
[26]E. W. Beier *et al.*, Phys. Rev. Lett. 37, 1117 (1976).
[27]L. Baum et al., Phys. Lett. 60B, 485 (1976); M. Barone et al., Nucl. Phys. B132, 29 (1978).
[28]V. Černý *et al.*, Acta Phys. Pol. B9, 269 (1978); Czech. J. Phys. B29, 1394 (1979); P. Lichard, Phys. Rev. D (to be published).